IEEE Access
Multidisciplinary | Rapid Review | Open Access Journal

Received August 26, 2021, accepted September 26, 2021, date of publication October 1, 2021, date of current version October 14, 2021.

Digital Object Identifier 10.1109/ACCESS.2021.3116938

Multicell AFE Rectifier Managed by Finite Control Set–Model Predictive Control

EDUARDO E. ESPINOSA[1], (Member, IEEE), PEDRO E. MELIN[2], (Member, IEEE), HUGO O. GARCÉS[3], (Member, IEEE), CARLOS R. BAIER[4], (Senior Member, IEEE), AND JOSÉ R. ESPINOZA[5], (Senior Member, IEEE)

[1]Department of Electrical Engineering, Faculty of Engineering, Universidad Católica de la Santísima Concepción, Concepción 4090541, Chile
[2]Department of Electrical and Electronic Engineering, Universidad del Bío-Bío, Concepción 4051381, Chile
[3]Department of Computer Science, Faculty of Engineering, Universidad Católica de la Santísima Concepción, Concepción 4090541, Chile
[4]Department of Electrical Engineering, Universidad de Talca, Curicó 3340000, Chile
[5]Department of Electrical Engineering, Universidad de Concepción, Concepción 4070386, Chile

Corresponding author: Eduardo E. Espinosa (eespinosa@ucsc.cl)

This work was supported in part by the Chilean Government under Research Project ANID/FONDECYT/11181203, Project ANID/FONDEQUIP/EQM140148, and Project ANID/FONDAP/SERC/15110019; and in part by the Universidad Católica de la Santísima Concepción From Dirección de Investigación under Grant FAA 02/2017.

ABSTRACT Multicell converters, based on power cells that use low-voltage semiconductors, implement AC motor drives for medium-and high-voltage applications. These converters feature an input multipulse transformer, which performs low-frequency harmonics cancelation generated by three-phase diode rectifiers in the power cells. Despite this advantage, the multipulse transformer is bulky, heavy, expensive, and must be designed according to the number of power cells required by a specific case, limiting the modularity of the topology. This work proposes a multicell converter based on power cells that requires a standard input transformer and uses active front-end rectifiers controlled by employing a finite control set-model predictive control algorithm. The proposed approach emulates the multipulse transformer harmonic cancelation owing to the predictive algorithm operation combined with input current references that are phase-shifted for each active front-end rectifier. Simultaneously, the DC voltages of the power cells are regulated and equalized among the cells using PI regulators. Experimental results confirm the feasibility of the proposed system as input currents in each Multicell AFE rectifier with a unitary displacement factor, and a low THD of 1.87% was obtained. It is then possible to replace the input multipulse transformer with standard ones while reducing the copper losses, reducing the K factor, and extending the modularity of the power cell to the input transformer.

INDEX TERMS Predictive control, ac–dc power converters, total harmonic distortion reduction.

I. INTRODUCTION

Medium AC drives based on multilevel converters have been increasingly applied in recent years [1]. For these applications, an inverter based on semiconductor devices with high blocking voltages can be used; however, multilevel converters allow to (*i*) improve the waveforms at the input and output of the power converter and (*ii*) to use low voltage/current power semiconductors, reducing cost and enhancing power converter reliability.

The multilevel converter has emerged as an alternative to the two-level inverter [2]. Within this category and voltage-source converters, there are three classic topologies, namely, neutral-point clamped (NPC) [3], cascade H-bridge (CHB) [4], and capacitor clamped [5]. These converters feature: (*i*) AC voltage with low distortion and low dv/dt, (*ii*) low switching frequency, and (*iii*) low common-mode voltage. These features allow the generation of medium-to-high voltage levels using low-rating semiconductors [6].

Cascaded H-bridge-based converters with symmetrical DC voltages are widely used in industrial applications [4]. This power topology is based on an input multipulse transformer, which feeds several three-phase to single-phase power cells. Each power cell uses a three-phase diode bridge rectifier, a DC voltage link based on a capacitor, and a single-phase voltage source inverter. Because of the diode rectifier, the input current in each power cell has an unwanted low-frequency harmonic content; however, from the viewpoint

The associate editor coordinating the review of this manuscript and approving it for publication was Mauro Gaggero.

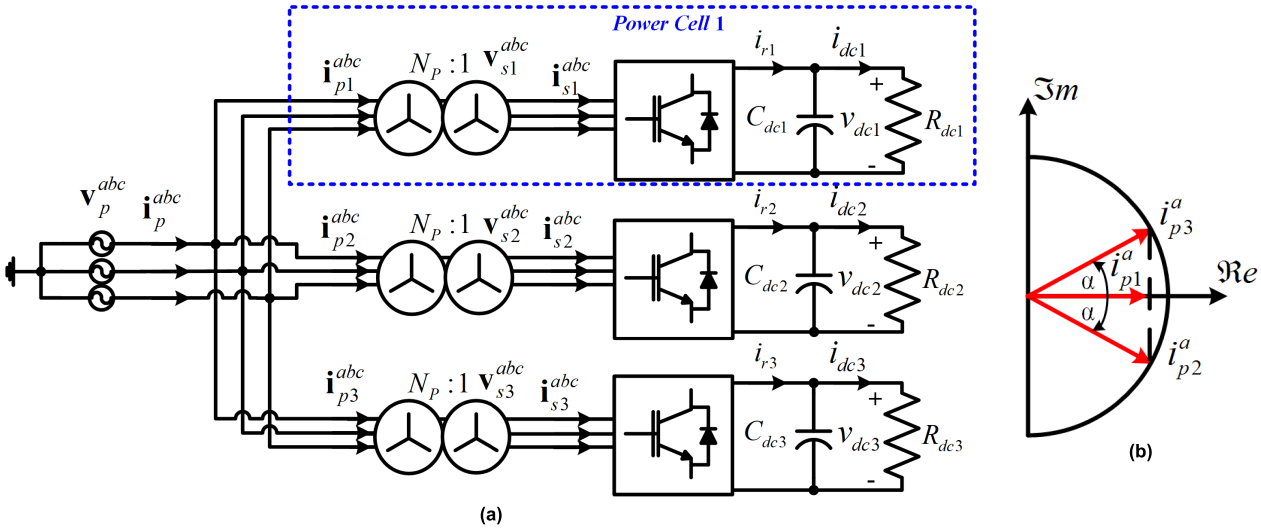

FIGURE 1. Topology and harmonic minimization scheme. (a) Multicell AFE rectifier with wye-wye transformers, (b) Phasor diagram of the input currents for the AFE rectifiers.

of the AC mains and because of the multipulse transformer, these harmonic components are canceled out, and therefore, they are not reflected in the transformer's primary overall current [7].

The literature reports multiple alternatives to improve the input current using sophisticated multipulse transformers [8], [9]. Other alternatives consider the use of modulating techniques developed especially for this type of topology using active front end (AFE) rectifiers [10]–[12]. Nevertheless, all these approaches require the use of a multipulse transformer, which must be designed according to the number of power cells used in each case, leading to a bulky and expensive transformer. Moreover, the AFE rectifier allows managing the active/reactive power flow and DC voltage control, for which various control strategies have been reported [13]–[16].

A control scheme that has been a matter of in-depth analyses in the last years is the model predictive control (MPC), which has been widely used in power converters [17]–[27]. This is due to the simple inclusion of nonlinearities and constraints; it uses the discrete nature of the power converters and provides a fast response to reference changes.

This work proposes the use of a control scheme based on finite control set-model predictive control [28] (FCS-MPC) for multicell converters based on AFE rectifiers [29]. The objectives are (*i*) the replacement of the input multipulse transformer for standard ones (in this case wye – wye transformers), reducing the copper losses and simplifying the transformer (K – Factor: 3,0), (*ii*) low-frequency harmonic cancelation in the overall AC input current, and (*iii*) regulation of the input displacement power factor and the DC voltage in every power cell. The FCS-MPC is used at the power cell level to reduce possible switch combinations and sufficient execution time. Each power cell receives an AC current reference template that has been optimized offline according to the number of power cells, and they are such that the THD of the overall AC current is minimized. Experimental results for three AFE rectifiers are presented to demonstrate the feasibility of the proposed control strategy, as shown in FIGURE 1.

This paper is organized as follows: Section II presents the mathematical development to determine the input current references of the power cells, concentrate the harmonic spectrum around 6 $n_c \pm 1$, and obtain a reduced THD in the input current of the AFE multicell rectifier. In Section III, the replacement of the input transformer is analyzed using standard IEEE/ANSI C57.18.10, standard UL 1561, and standard IEEE/ANSI C57.110. Then, in Section IV, the mathematical model for a power cell is obtained, which is necessary for the FCS – MPC, which is used in Section V to synthesize the master-slave control scheme, which must be used in each power cell; in Section VI, the satisfactory experimental results obtained in a low-power prototype are presented. Finally, in Section VII, the conclusions of this study are detailed.

II. HARMONIC MINIMIZATION

The FCS-MPC has the flexibility to operate with current or voltage references with fast dynamics and proper tracking [20], which makes this strategy suitable for input current control in AFE rectifiers. In this work, the topology is shown in FIGURE 1(a), which is composed of three-phase wye-to-wye transformers. Each secondary feeds an AFE, which has a DC link capacitor to hold the voltage, and a resistive load is considered for simplicity. The analysis in this study was performed for three power cells, $n_c = 3$.

The choice of $n_c = 3$ is based on the following: Input transformer with reduced K-factor, compared to a multipulse transformer. Unfortunately, the use of FCS-MPC in the input current control with a sinusoidal reference generates

a dispersed harmonic spectrum [28], possibly generating resonance in the AC network. This allows the use of input current references with known harmonics in each power cell ($6\ n_c \pm 1 = 17^{\text{th}}$ and 19^{th} harmonics) to obtain a fixed and known harmonic spectrum despite the use of FCS-MPC in control of the input current. For the above to be valid, $n_c \geq 3$ must be fulfilled to obtain an input transformer whose construction, cost, and design are more straightforward than a multipulse transformer.

Consequently, the reference currents include harmonics 17^{th} and 19^{th}, aimed at fixing the harmonic content of the input current of each AFE rectifier, avoiding a dispersed spectrum as typically found when using the FCS – MPC with a high sampling time and sinusoidal references in the input current loop of the AFE rectifier.

However, these harmonics (17^{th} and 19^{th}) are not desired in the total input current of the multicell AFE rectifier. Hence, the input current reference for each AFE rectifier has a phase angle α at the fundamental frequency, as shown in FIGURE 1(b). This angle is calculated offline to obtain the minimum THD in the total input current of the multicell AFE rectifier.

The THD minimization considers the fundamental components of the current, as shown in FIGURE 1(b), where the phase shift angle α is responsible for allowing harmonic minimization. This angle is computed offline to obtain an overall input current $\mathbf{i}_p^{abc}$ with a minimum THD.

Therefore, to calculate the phase shift angle α, it is necessary to characterize the currents in the secondary winding of the transformer. This characterization is performed for phase a, as it is valid for phases b and c.

The input current for rectifier 1, referred to as the primary winding of the transformer, is given by:

$$i_{p1}^{a}(t) = \frac{I\cos(\alpha)}{N_P}\left[\sin(\omega t) - \frac{\sin(17\cdot\omega t)}{17} - \frac{\sin(19\cdot\omega t)}{19}\right], \tag{1}$$

Then, the input current for rectifier 2, referred to as the primary, is:

$$i_{p2}^{a}(t) = \frac{I}{N_P}\left[\sin(\omega t - \alpha) - \frac{\sin(17\cdot\omega t - 17\cdot\alpha)}{17} - \frac{\sin(19\cdot\omega t - 19\cdot\alpha)}{19}\right], \tag{2}$$

Thus, the input current for rectifier 3, referred to as the primary transformer, is:

$$i_{p3}^{a}(t) = \frac{I}{N_P}\left[\sin(\omega t + \alpha) - \frac{\sin(17\cdot\omega t + 17\cdot\alpha)}{17} - \frac{\sin(19\cdot\omega t + 19\cdot\alpha)}{19}\right], \tag{3}$$

Assuming that the transformer's turns ratio is unitary ($N_P = 1$), the overall input current for phase a is given by

$$i_p^a(t) = \frac{I}{N_P}\begin{bmatrix} 3\cos(\alpha)\sin(\omega t) \\ -\dfrac{\sin(17\cdot\omega t)\,[\cos(\alpha) + 2\cos(17\cdot\alpha)]}{17} \\ -\dfrac{\sin(19\cdot\omega t)\,[\cos(\alpha) + 2\cos(19\cdot\alpha)]}{19} \end{bmatrix}. \tag{4}$$

Therefore, considering that the THD for any waveform is given by,

$$THD(I) = \frac{\sqrt{\sum_{k=2}^{n=51} I_k^2}}{I_1} \times 100, \tag{5}$$

Then, the THD expression of the total input current i_p^a, to obtain the value of α, which attenuates the harmonics 17^{th} and 19^{th} is

$$THD\left(i_p^a\right) = \frac{\sqrt{\left(\frac{\cos(\alpha)+2\cdot\cos(17\cdot\alpha)}{17}\right)^2 + \left(\frac{\cos(\alpha)+2\cdot\cos(19\cdot\alpha)}{19}\right)^2}}{3\cdot\cos(\alpha)} \times 100 \tag{6}$$

wherein the following constraint is considered,

$$0 \leq \alpha \leq {}^{\pi}/_{2} \tag{7}$$

As a result of the minimization process, a phase shift angle $\alpha = 6.671°$ was obtained, and the overall current system i_p^a achieved a total THD of 0.561 %. This minimization was performed in MatLab®using the fmincon command to minimize the nonlinear expressions using constraints.

Then, using the obtained α through THD minimization in (1), (2) and (3), we obtain the waveforms of the input current references of the power cells, as shown in FIGURE 2(a)–(c), which will be used in the input current loop managed by FCS-MPC. Finally, the amplitude of the waveforms is given by the output V_{DC} PI controller.

The waveforms of input currents in the AFE rectifiers (FIGURE 2(a)–(c)) are consistent as they contain the 17^{th} and 19^{th} harmonics, which are not present in the overall input current of the multicell rectifier because the value of α is calculated to minimize the resulting harmonics (FIGURE 2(d)) in the AC input overall current $\mathbf{i}_p^{abc}$.

The use of FCS – MPC with a current reference that imposes a fixed harmonic spectrum, as the proposed 18 pulses type of waveform, overcomes some of the problems of the FCS – MPC approach, such as the spread harmonic spectrum. This is because the resulting current harmonics are around a known frequency, which avoids potential harmful effects on the AC power system, such as resonances. Similarly, the proposed harmonic minimization allows the modularity of the power cell to be extended to the input transformer with a more straightforward design.

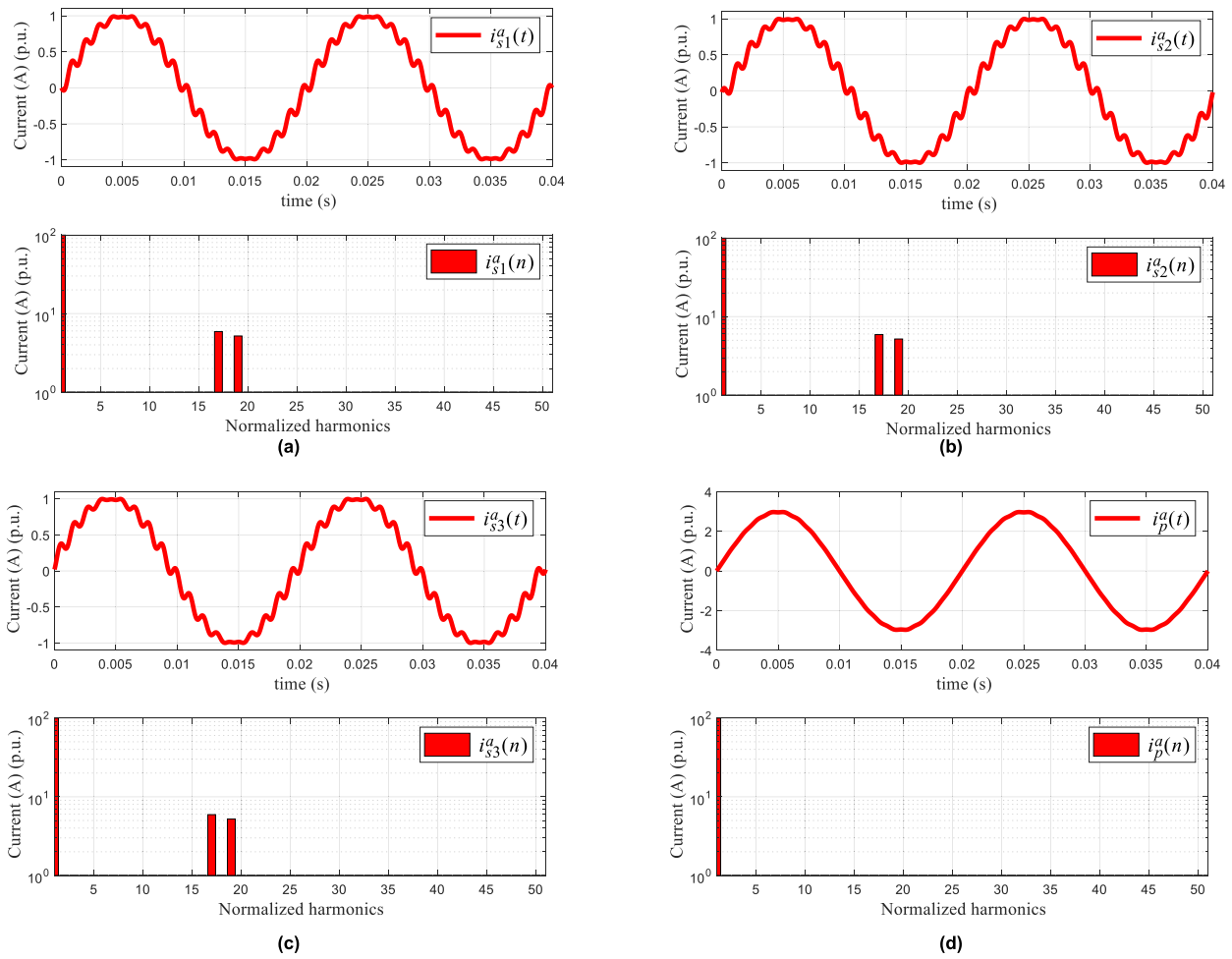

FIGURE 2. Input current references and harmonic content AFE rectifier for phase a. (a) AFE rectifier 1, (b) AFE rectifier 2, (c) AFE rectifier 3, (d) Multicell AFE rectifier input current.

III. TRANSFORMER REPLACEMENT

In this study, we propose to replace the input multipulse transformer with a more straightforward design transformer. In this case, a wye – wye transformer, leaving the harmonic task cancelation at the input current loop in each power cell and allowing extended modularity to the traditional power cell, considering the input transformer.

The input transformer replacement was evaluated considering two criteria: (*i*) transformer losses, standard IEEE/ANSI C57.18.10 [30], and (*ii*) K-factor, standard UL 1561[31] and standard IEEE/ANSI C57.110 [32].

A. TRANSFORMER LOSSES

The transformer losses are defined as,

$$P_T = P_{NL} + P_{LL}. \tag{8}$$

where P_{NL} is associated with the core excitation voltage or no-load losses, P_{LL} is associated with the load losses, and P_T is the total transformer loss.

The load losses are defined as,

$$P_{LL} = P_{DC} + P_{EC} + P_{OSL}, \tag{9}$$

where P_{DC} is associated with copper losses, P_{EC} is associated with eddy current losses, and P_{OSL} is the loss to the transformer structure. Therefore, if a nonsinusoidal current flows in a transformer, it is necessary to redefine it (9), considering the harmonic loss factors F_{HL-WE} and F_{HL-OSL}.

$$P_{LL} = I_P'^2 R_P + I_S'^2 R_S + P'_{EC} + P'_{OSL}, \tag{10}$$

where $P'_{EC} = (P_{EC-P} + P_{EC-S}) \cdot F_{HL-WE}$ and $P'_{OSL} = (P_{OSL-P} + P_{OSL-S}) \cdot F_{HL-OSL}$. In addition, I'_P is the primary current RMS value, I'_s is the secondary current RMS value, R_P is the resistance of the primary winding, and R_S is the resistance of the secondary winding.

B. K–FACTOR

K is the transformer's capacity to work with nonlinear loads. It is a way of quantifying the heating produced in transformers when harmonics occur due to the presence of nonlinear loads. To compute this value, it is necessary to know the harmonic content of the current through the transformer. K: Factor is

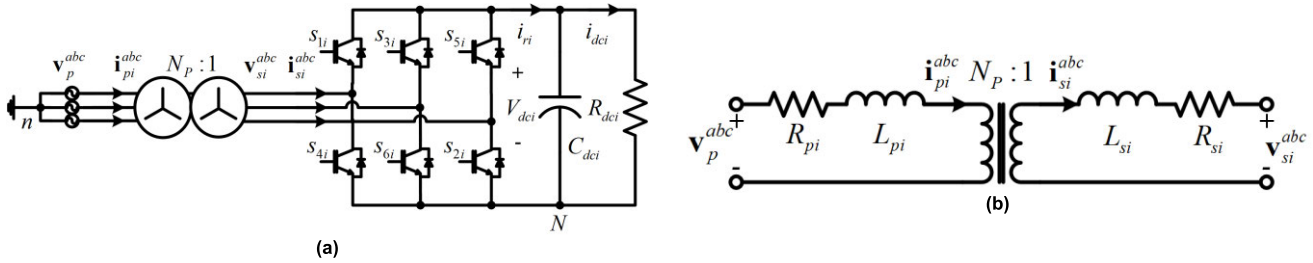

FIGURE 3. Power cell in multicell AFE rectifier. (a) AFE rectifier connected the wye-wye transformer, (b) wye-wye transformer model.

defined as

$$K - Factor = \sum_{h} \left(\frac{I_{rms \cdot h}}{I_{rms}} \right)^2 h^2. \tag{11}$$

Transformers are typically designed with K factors equal to 1, 4, 9, 13, 30, 40, and 50. A transformer whose current flowing through it is perfectly sinusoidal has a K factor of 1. Transformers that operate in distribution systems with a high harmonic content can present problems owing to the increase in temperature due to the circulation of these harmonics. In this situation, the transformer must not operate at its rated power, and the load must be reduced (derating).

C. TRANSFORMER COMPARISON

A multipulse transformer for $n_c = 3$ power cells is considered for this comparison, with a phase shift in the secondary windings of $\pm 20°$. On the other hand, the proposed topology uses a wye – wye transformer.

In the proposed topology, specifically in the secondary winding of the wye – wye transformer, we have 17^{th} and 19^{th} harmonics. As a result, the RMS value of the current in the secondary winding is 1.003 p.u. Similarly, in the secondary windings of the multipulse transformer, the RMS value of the current in the secondary winding is 1.043 p.u., TABLE 1. Thus, it is possible to obtain a 7.52% reduction in the copper losses at the secondary winding of the transformer.

From the harmonic spectra in the primary and secondary windings, TABLE 1 computed the harmonic loss factors F_{HL-WE}, F_{HL-OSL}, and K – Factor for the comparison.

For both input transformers, F_{HL-WE} is the same. However, the F_{HL-OSL} is different, particularly when the wye – wye transformer is reduced by 26.75%.

Finally, comparing the K – factor in both transformers, the wye – wye transformer is low (3,00) owing to the current harmonics. Thus, by the more straightforward design of the transformer, we have a cost reduction and less complicated design.

IV. AFE RECTIFIER MODEL

The previous waveforms shown in FIGURE 2(a)–(c) are used as references for the input current control of each AFE rectifier. A control scheme with a high wideband must be used to ensure that the harmonics current (17^{th} and 19^{th}) will be generated with a well-defined amplitude and phase. In this work, the FCS – MPC is used, which requires a system model to predict the input current, and the circuit depicted in FIGURE 3(a) is used to obtain a model for the input current of an AFE rectifier.

One issue to consider is the use of a wye-wye transformer between the AFE rectifier and the AC source. Therefore, a model referred to as the primary winding of the transformer is preferred because it is easier to formulate the FCS – MPC algorithm. In addition, the modeling of the transformer magnetizing branch can be neglected because the magnitude of the magnetization current is low.

Then, by applying the Kirchhoff voltage law in FIGURE 3(b), we obtain

$$\mathbf{v}_p^{abc} = R_p \mathbf{i}_{pi}^{abc} + L_p \frac{d\mathbf{i}_{pi}^{abc}}{dt} + N_P^2 R_s \mathbf{i}_{pi}^{abc} + N_P^2 L_s \frac{d\mathbf{i}_{pi}^{abc}}{dt} + N_P \mathbf{v}_{si}^{abc}, \tag{12}$$

where $\mathbf{v}_{si}^{abc}$ is,

$$\mathbf{v}_{si}^{abc} = \mathbf{M}\mathbf{s}_i^{abc} V_{DCi} = \frac{1}{3} \begin{bmatrix} 2 & -1 & -1 \\ -1 & 2 & -1 \\ -1 & -1 & 2 \end{bmatrix} \mathbf{s}^{abc} V_{DCi}, \tag{13}$$

Thus, by replacing (13) in (12) and obtaining the state variable $\mathbf{i}_p^{abc}$,we obtain

$$\frac{d\mathbf{i}_{pi}^{abc}}{dt} = \frac{1}{\left(L_p + N_P^2 L_s\right)} \left[\mathbf{v}_p^{abc} - \left(R_p + N_P^2 R_s \right) \mathbf{i}_{pi}^{abc} - N_P \mathbf{M}\mathbf{s}_i^{abc} V_{DCi} \right]. \tag{14}$$

Finally, (14) shows the model for the input current that is valid for a balanced AC source.

The model obtained in the continuous-time domain was then discretized to use it with the FCS-MPC. In the technical literature [33], we find numerous discretization methods: forward and backward Euler, Tustin, and accurate discretization. In this case, because the sample time is short ($\approx 55\ \mu$S), it is possible to consider discretization using the forward Euler method.

TABLE 1. Harmonic spectra in input transformers.

Harmonic order (h)	Multipulse Transformer 18 Pulses			Wye- Wye Transformer		
	P.U. load current secondary	P.U. flux secondary	P.U. load current and flux primary	P.U. load current secondary	P.U. flux secondary	P.U. load current and flux primary
1	1,000	1,000	1,000	1,000	1,000	1,000
5	0,200	0,000	0,000	0,000	0,000	0,000
7	0,143	0,000	0,000	0,000	0,000	0,000
11	0,091	0,000	0,000	0,000	0,000	0,000
13	0,077	0,000	0,000	0,000	0,000	0,000
17	0,059	0,059	0,059	0,059	0,059	0,059
19	0,053	0,053	0,053	0,053	0,053	0,053
23	0,043	0,000	0,000	0,000	0,000	0,000
25	0,040	0,000	0,000	0,000	0,000	0,000
Total	1,041		1,003	1,003		1,003
$F_{HL\text{-}WE}$		2,98	2,98		2,98	2,98
$F_{HL\text{-}OSL}$	1,451			1,063		
$K-Factor$	8,30→9,00		3,00→4,00	3,00→4,00		3,00→4,00

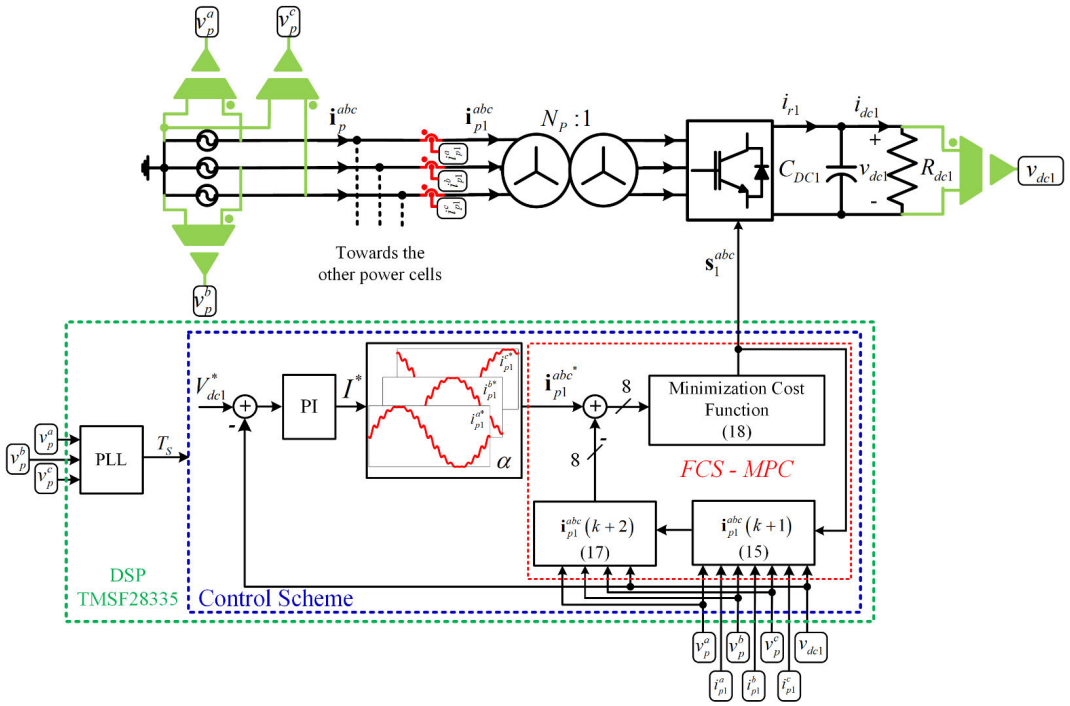

FIGURE 4. Control scheme in each power cell.

Then, the discrete model for the input current of the AFE rectifier, referred to as the primary winding transformer, is obtained as

$$\mathbf{i}_{pi}^{abc}(k+1)=\left[1-\frac{(R_p+N_P^2R_s)}{(L_p+N_P^2L_s)}T_s\right]\mathbf{i}_{pi}^{abc}(k)+\left[\mathbf{v}_p^{abc}(k)-N_P\mathbf{M}\mathbf{s}_i^{abc}V_{DCi}(k)\right]\frac{T_s}{(L_p+N_P^2L_s)}. \quad (15)$$

This allows us to predict future behavior from the previous state and system inputs.

V. CONTROL SCHEME

The current control of the AFE rectifiers is performed using FCS – MPC because of its ability to follow the reference fairly accurately and quickly, while regulating the DC voltage; an outer linear PI controller is used, as shown in FIGURE 4.

The FCS-MPC used is the conventional one, with delay compensation by calculation, as used in [34], [35].

The PI controller regulates the DC voltage V_{DC}, which gives the amplitude of the input current reference for the AFE rectifier. It is formulated in [24] by an amplitude model; this control loop is possible because the transfer function between

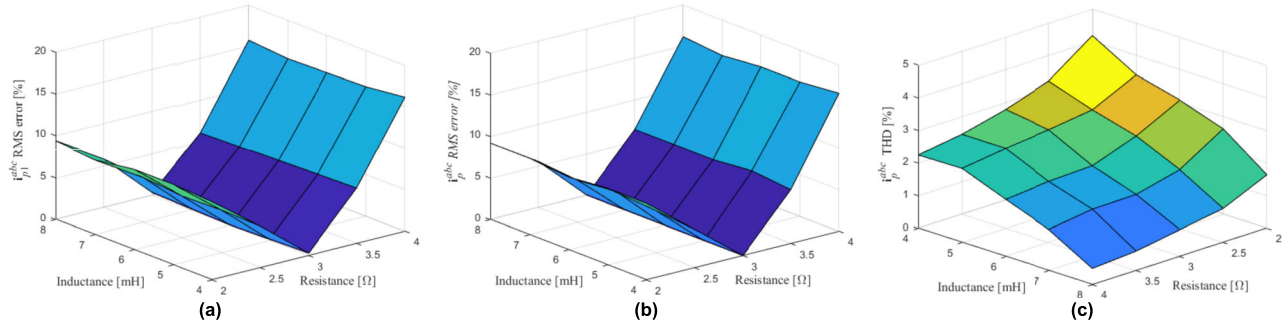

FIGURE 5. Parameter analysis. (a) i_{p1}^{abc} RMS error, (b) i_{p}^{abc} RMS error, (c) i_{p}^{abc} THD variation.

I_{pi} and V_{DCi} is

$$\frac{V_{dci}(s)}{I_{pi}(s)} = \frac{-3L_{pi}I_{pi}}{2C_{dci}V_{dci}} \frac{\left(s - \left(\frac{V_{pi}\cos(\phi)}{L_{pi}I_{pi}} - \frac{2R_{pi}}{L_{pi}}\right)\right)}{\left(s + \frac{2}{R_{dci}C_{dci}}\right)}. \quad (16)$$

The current reference amplitude enters the current reference generation block, which also considers the phase-shift angle α. Once the current reference is generated, it is compared with the estimation made by the FCS-MPC algorithm, which considers the delay compensation for calculation. Thus, rewriting (15) for the instant $k+2$ yields

$$\begin{aligned}\mathbf{i}_{pi}^{abc}(k+2) &= \left[1 - \frac{\left(R_p + N_P^2 R_s\right)}{\left(L_p + N_P^2 L_s\right)} T_s\right] \mathbf{i}_{pi}^{abc}(k+1) \\ &+ \left[\mathbf{v}_p^{abc}(k+1) - N_P \mathbf{M}\mathbf{s}_i^{abc} V_{DCi}(k+1)\right] \frac{T_s}{\left(L_p + N_P^2 L_s\right)}. \end{aligned} \quad (17)$$

From (17) some approximations can be made, such as $\mathbf{v}_p^{abc}(k+1) \approx \mathbf{v}_p^{abc}(k)$, $V_{DCi}(k+1) \approx V_{DCi}(k)$, because the sample time is short compared to the dynamics of these variables.

Finally, among all the valid switch states of the AFE rectifier, a switch state is chosen that minimizes the cost function, defined as

$$g(k+2) = \sum_{j=a}^{c} \left| i_p^{j^*}(k) - i_p^{j}(k+2) \right|. \quad (18)$$

Functional (18) corresponds to the input current control of the AFE rectifier, where the reference $i_p^{j^*}(k)$ and estimated input currents $i_p^{j}(k+2)$are necessary. Thus, a single state is selected for each rectifier within eight possible states, minimizing the function.

VI. SENSITIVITY ANALISYS

Owing to the nonlinear nature of the FCS-MPC, it is not possible to analyze it using linear tools as the locus of the roots, making it difficult to analyze the stability. This analysis focused on the behavior of the controller.

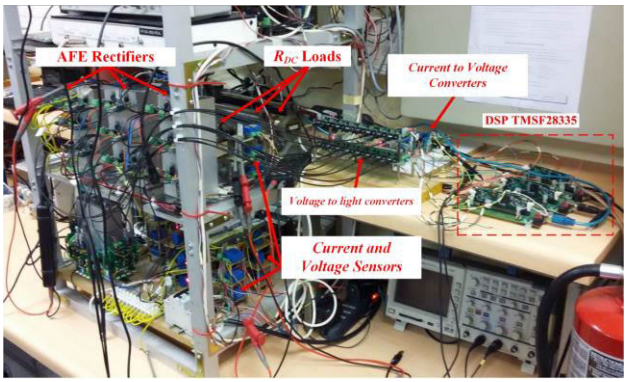

FIGURE 6. Experimental setup.

Thus, a variation of the parameters input transformer, R_p, R_s, L_p, and L_s, follows from (15) and (17). Therefore, it can be deduced that any change in R_p and R_s affects the current direction of the current. On the other hand, before a change in L_p and L_s, it affects the direction of the possible eight possible states of the rectifier PWM voltage and the current direction of the current. Therefore, a priori, it can be deduced that a change in the parameters of L_p and L_s will have a more significant effect on the behavior of the FCS-MPC.

FIGURE 5(a) shows the input current variation in a power cell, and FIGURE 5(b) shows the variation in the input current of the multicell AFE rectifier. The most significant current error occurs when L_p, L_s, and R_p, R_s increase in both cases. In particular, this variation affects prediction (17) owing to the use of computational delay compensation. The variation in parameters affects (15) and (17). On the other hand, the variation of parameters causes the THD of the input current to change; FIGURE 5(c) shows that before an increase in L_p and L_s, a decrease in THD is achieved, which is expected.

VII. EXPERIMENTAL RESULTS

A three-power-cell-based experimental prototype was assembled to test the proposed control scheme and current templates. The prototype is depicted in FIGURE 6 and uses three DSP TMSF28335 to control an AFE rectifier in a dedicated manner. For the correct application of the phase

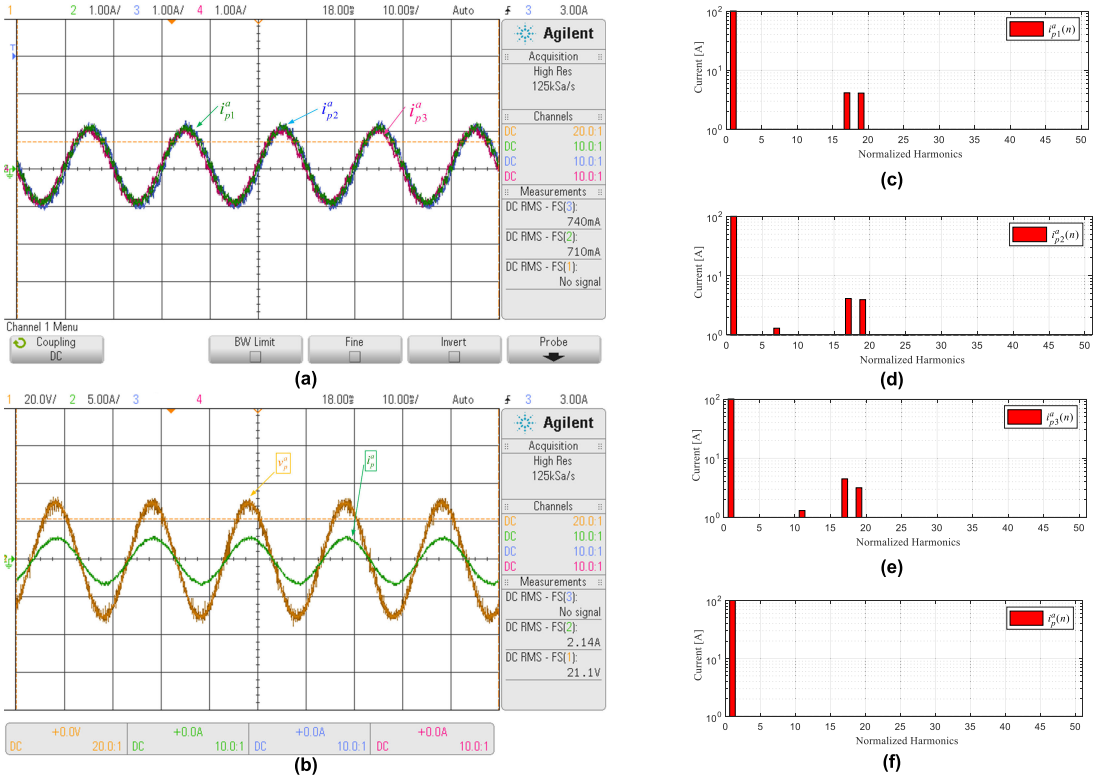

FIGURE 7. Experimental key results, input current loop. (a) Input current power cell phase *a* $i_{p_1}^a$, $i_{p_2}^a$ and $i_{p_3}^a$ (b) AC grid voltage (yellow) and input current multicell AFE rectifier (green) (c) harmonic spectrum $i_{p_1}^a$, (d) harmonic spectrum $i_{p_2}^a$, (e) harmonic spectrum $i_{p_3}^a$, (f) harmonic spectrum input current multicell AFE rectifier.

shift angle α, good synchronization with the AC network is necessary through a PLL [36], [37], FIGURE 4.

The experimental parameters are shown in TABLE 2.

TABLE 2. Experimental parameters.

Symbol	Quantity	Value
V_P	Phase voltage	31.1[V]
f	Network frequency	50 [Hz]
R_p	Transformer prim. resistance	3 [Ω]
L_p	Transformer prim. Inductance.	6 [mH]
R_p	Transformer sec. resistance	3 [Ω]
L_p	Transformer sec. Inductance.	6 [mH]
N_P	Turns ratio	1
α	Phase shift angle.	6.671°
R_{DC}	DC load resistance.	89 [Ω]
C_{DC}	DC link capacitor	4.7[mF]
V_{DC}	DC link voltage	55 [V]
T_S	Sample time	55.56[μS]
K_P	Proportional Gain	0.8
T_i	Integral time	0.02

A. INPUT CURRENT LOOP

The control scheme is shown in FIGURE 4. One of its objectives is to correctly manipulate the input currents of the power cells to achieve harmonic compensation. The implementation of the input current control loop for the AFE rectifiers, based on FCS-MPC, is presented in FIGURE 7. It is appreciated that these input currents have a distortion, as shown in FIGURE 7(a), owing to the harmonics imposed by the current references.

In addition, they have a phase shift between them, the angle α, which leads to harmonic compensation in the transformer input currents. This is consistent with the mathematical modeling of the input current waveform in the AFE rectifiers (1)–(3). FIGURE 7(c)–(e) show that the input current harmonic spectrum of the AFE rectifiers contains harmonics 17th and 19th, which is consistent with what is shown in FIGURE 2(a)-(c).

The input currents of the power cell contain the harmonics 17th and 19th; these harmonics contain a phase shift given by the angle α, which fulfills four objectives: (*i*) to fix the harmonic content of the input currents of the AFE rectifiers, improving the drawback that has the FCS – MPC, spread harmonic spectrum (*ii*) due to the use of three cells, the harmonic compensation of the currents is made to emulate a rectifier of 18 pulses, but achieving a low THD of 1.87%; (*iii*) the fact of being modular equipment allows the generation of an input current with low THD, from currents with lower quality, and (*iv*) replace the input transformer with a more straightforward design. FIGURE 7(b) shows that the input voltage and current of the multicell AFE rectifier are in phase; hence, the unitary displacement power factor is achieved. In addition, the AC grid current does not contain the harmonics 17th and 19th, as shown in FIGURE 7(f). This

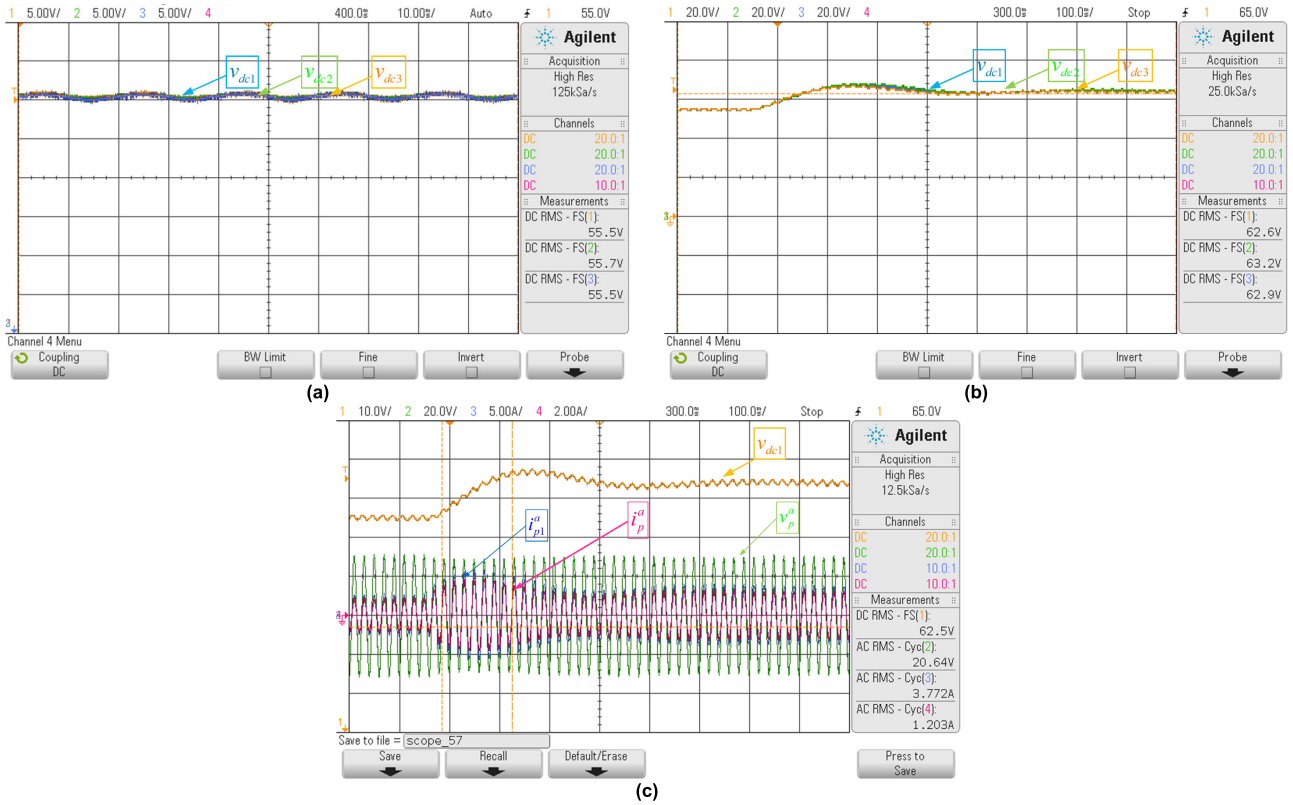

FIGURE 8. Experimental key results, dc voltage loop. (a) Steady state performance, (b) Dynamic response performance, (c) Reference change in the current loop by reference change in the dc voltage loop.

is due to the calculation of the angle α. Finally, the THD of the multicell AFE rectifier input current $\mathbf{i}_p^{abc}$ is 1.87%.

B. DC VOLTAGE LOOP

The performance of the PI linear controller for the DC voltage in each power cell at steady-state and dynamic behavior facing a step-change in the reference is reviewed.

The AFE rectifier DC voltage link is a nonlinear system, and to design a PI linear controller, it must be linearized to obtain a transfer function between the DC voltage link and the input current of the AFE rectifier (16).

FIGURE 8(a) shows the excellent regulation of the DC-link voltage in the power cells. The DC voltage references are set at 55 V, where the DC voltage link follows the reference, and the ripple is approximately 2%. The ripple in the DC voltage is due to a second harmonic in the input current because of the number of points used per period and tracking the input current reference, generating fundamental frequency harmonics in the i_{ri} current, which is not reduced by the capacitive filter on the DC side.

In the same way, the 17th and 19th harmonics, including the input current, do not affect the DC voltage behavior.

To observe the dynamic response for a step-change reference, a change of 10 V was made, from 55 to 65 V, as shown in FIGURE 8(b). Again, the response achieved was satisfactory, with an overshoot close to 5% and a settling time of approximately 300 ms (Table 2).

The control scheme used in each power cell is of the master-slave type; therefore, any change in the DC voltage link will affect the input current of the power cell i_{p1}^a and the input current of the multicell AFE rectifier i_p^a. This is observed in FIGURE 8(c), where the DC 1 voltage is subjected to a step-type change from 55 to 65 V. Consequently, the input current phase in the power cell one increases, as well as the input current of the multiphase rectifier AFE phase *a*.

In addition, when the system stabilizes, the AC supply voltage and the multicell AFE rectifier input current, phase *a*, are maintained in phase. Finally, the quality of this current remains the same because the minimization performed is based on the THD, independent of the amplitude of the waveform.

VIII. CONCLUSION

This work shows that it is possible to replace the multipulse transformer in a multicell converter with one less complex (wye-wye transformer), obtaining a 7.52% reduction in the copper losses in the secondary winding, a 26.75% reduction in F_{HL-OSL}, and a less complicated design with a K-factor of 3,00. This is achieved by replacing the diode-based power cells with active front-end-based power cells using a model predictive control algorithm.

A minimization strategy for the input current harmonic for a multicell AFE rectifier is presented. This minimization performs the offline calculation of the input current reference

waveform needed for the FCS-MPC algorithm in the AFE rectifiers, which considers a phase shift angle α. This angle is calculated to minimize the multicell AFE rectifier input current THD and obtain a unitary displacement power factor. Thus, the harmonic minimization task is no longer performed by the input multipulse transformer, but is performed by the control scheme.

The reference of the input current waveform of each power cell, which contains the angle α and is calculated offline, defines the harmonic content (17^{th} and 19^{th}) of this current. Thus, overcoming the drawback of the FCS-MPC, the spread spectrum, and canceling these harmonics so that they do not appear in the AC network, resulting in a low THD (1.87%).

Because the harmonic cancelation task is transferred to the control scheme, the wye-wye input transformer becomes part of the power cell. Hence, the power cell is now formed by a three-phase wye-to-wye transformer, an AFE rectifier, and a single-phase inverter; in this case, it is replaced by a resistive load.

The sensitivity analysis of the input transformer parameters shows that the method is still valid before variations of 33%.

The experimental results confirm the excellent performance of the proposed control scheme. Furthermore, although the results are provided for three AFE rectifiers, the methodology can be extended to an arbitrary number of power cells.

REFERENCES

[1] H. Akagi, "Multilevel converters: Fundamental circuits and systems," *Proc. IEEE*, vol. 105, no. 11, pp. 2048–2065, Nov. 2017, doi: 10.1109/JPROC.2017.2682105.

[2] J. I. Leon, S. Kouro, L. G. Franquelo, J. Rodriguez, and B. Wu, "The essential role and the continuous evolution of modulation techniques for voltage-source inverters in the past, present, and future power electronics," *IEEE Trans. Ind. Electron.*, vol. 63, no. 5, pp. 2688–2701, May 2016, doi: 10.1109/TIE.2016.2519321.

[3] A. Nabae, I. Takahashi, and H. Akagi, "A new neutral-point-clamped PWM inverter," *IEEE Trans. Ind. Appl.*, vol. IA-17, no. 5, pp. 518–523, Sep. 1981, doi: 10.1109/TIA.1981.4503992.

[4] P. W. Hammond, "A new approach to enhance power quality for medium voltage AC drives," *IEEE Trans. Ind. Appl.*, vol. 33, no. 1, pp. 202–208, Jan./Feb. 1997, doi: 10.1109/28.567113.

[5] J.-S. Lai and F. Z. Peng, "Multilevel converters-a new breed of power converters," *IEEE Trans. Ind. Appl.*, vol. 32, no. 3, pp. 509–517, May/Jun. 1996, doi: 10.1109/28.502161.

[6] J. Rodriguez, L. G. Franquelo, S. Kouro, J. I. Leon, R. C. Portillo, M. A. M. Prats, and M. A. Perez, "Multilevel converters: An enabling technology for high-power applications," *Proc. IEEE*, vol. 97, no. 11, pp. 1786–1817, Nov. 2009, doi: 10.1109/JPROC.2009.2030235.

[7] D. A. Paice, *Power Electronics Converter Harmonics: Multipulse Methods for Clean Power*. Hoboken, NJ, USA: Wiley, 1999.

[8] B. Singh, S. Gairola, B. N. Singh, A. Chandra, and K. Al-Haddad, "Multipulse AC–DC converters for improving power quality: A review," *IEEE Trans. Power Electron.*, vol. 23, no. 1, pp. 260–281, Jan. 2008, doi: 10.1109/TPEL.2007.911880.

[9] J. Wang and Y. Li, "PWM rectifier in power cell of cascaded H-bridge multilevel converter," in *Proc. Int. Conf. Electr. Mach. Syst. (ICEMS)*, Seoul, South Korea, Oct. 2007, pp. 18–21.

[10] A. Xu and S. Xie, "A multipulse-structure-based bidirectional PWM converter for high-power applications," *IEEE Trans. Power Electron.*, vol. 24, no. 5, pp. 1233–1242, May 2009, doi: 10.1109/TPEL.2008.2011738.

[11] B. H. Sun, "High voltage regenerative converter and the control of its PWM rectifier," in *Proc. Int. Conf. E-Product E-Service E-Entertainment*, Henan, China, Nov. 2010, pp. 1–4, doi: 10.1109/ICEEE.2010.5661257.

[12] J. A. Pontt, J. R. Rodriguez, A. Liendo, P. Newman, J. Holtz, and J. M. S. Martin, "Network-friendly low-switching-frequency multipulse high-power three-level PWM rectifier," *IEEE Trans. Ind. Electron.*, vol. 56, no. 4, pp. 1254–1262, Apr. 2009, doi: 10.1109/TIE.2008.2007998.

[13] T. G. Habetler, "A space vector-based rectifier regulator for AC/DC/AC converters," *IEEE Trans. Power Electron.*, vol. 8, no. 1, pp. 30–36, Jan. 1993, doi: 10.1109/63.208497.

[14] G. Brando, A. Dannier, and A. Del Pizzo, "An optimized control technique of cascaded H-bridge multilevel active front-ends," in *Proc. 12th Int. Power Electron. Motion Control Conf.*, Portorož, Slovenia, Aug. 2006, pp. 793–799, doi: 10.1109/EPEPEMC.2006.4778496.

[15] M. Malinowski, M. P. Kazmierkowski, and A. M. Trzynadlowski, "A comparative study of control techniques for PWM rectifiers in AC adjustable speed drives," *IEEE Trans. Power Electron.*, vol. 18, no. 6, pp. 1390–1396, Nov. 2003, doi: 10.1109/TPEL.2003.818871.

[16] J. R. Rodriguez, J. W. Dixon, J. R. Espinoza, J. Pontt, and P. Lezana, "PWM regenerative rectifiers: State of the art," *IEEE Trans. Ind. Electron.*, vol. 52, no. 1, pp. 5–22, Feb. 2005, doi: 10.1109/TIE.2004.841149.

[17] A. Linder and R. Kennel, "Model predictive control for electrical drives," in *Proc. IEEE 36th Conf. Power Electron. Spec.*, Recife, Brazil, Jun. 2005, pp. 1793–1799, doi: 10.1109/PESC.2005.1581874.

[18] R. Kennel, A. Linder, and M. Linke, "Generalized predictive control (GPC)-ready for use in drive applications?" in *Proc. IEEE 32nd Annu. Power Electron. Spec. Conf.)*, vol. 4, Vancouver, BC, Canada, Jun. 2001, pp. 1839–1844, doi: 10.1109/PESC.2001.954389.

[19] P. Cortes, M. P. Kazmierkowski, R. M. Kennel, D. E. Quevedo, and J. Rodriguez, "Predictive control in power electronics and drives," *IEEE Trans. Ind. Electron.*, vol. 55, no. 12, pp. 4312–4324, Dec. 2008, doi: 10.1109/TIE.2008.2007480.

[20] S. Kouro, P. Cortes, R. Vargas, U. Ammann, and J. Rodriguez, "Model predictive control—A simple and powerful method to control power converters," *IEEE Trans. Ind. Electron.*, vol. 56, no. 6, pp. 1826–1838, Jun. 2009, doi: 10.1109/TIE.2008.2008349.

[21] S. Vazquez, J. Rodriguez, M. Rivera, L. G. Franquelo, and M. Norambuena, "Model predictive control for power converters and drives: Advances and trends," *IEEE Trans. Ind. Electron.*, vol. 64, no. 2, pp. 935–947, Feb. 2017, doi: 10.1109/TIE.2016.2625238.

[22] P. Cortés, J. Rodríguez, P. Antoniewicz, and M. Kazmierkowski, "Direct power control of an AFE using predictive control," *IEEE Trans. Power Electron.*, vol. 23, no. 5, pp. 2516–2523, Sep. 2008, doi: 10.1109/TPEL.2008.2002065.

[23] H. A. Young, V. A. Marin, C. Pesce, and J. Rodriguez, "Simple finite-control-set model predictive control of grid-forming inverters with LCL filters," *IEEE Access*, vol. 8, pp. 81246–81256, 2020, doi: 10.1109/ACCESS.2020.2991396.

[24] M. A. Perez, R. Lizana Fuentes, and J. Rodríguez, "Predictive control of DC-link voltage in an active-front-end rectifier," in *Proc. IEEE Int. Symp. Ind. Electron.*, Gdańsk, Poland, Jun. 2011, pp. 1811–1816, doi: 10.1109/ISIE.2011.5984432.

[25] Y. Yang, H. Wen, and D. Li, "A fast and fixed switching frequency model predictive control with delay compensation for three-phase inverters," *IEEE Access*, vol. 5, pp. 17904–17913, 2017, doi: 10.1109/ACCESS.2017.2751619.

[26] P. Zanchetta, D. B. Gerry, V. G. Monopoli, J. C. Clare, and P. W. Wheeler, "Predictive current control for multilevel active rectifiers with reduced switching frequency," *IEEE Trans. Ind. Electron.*, vol. 55, no. 1, pp. 163–172, Jan. 2008, doi: 10.1109/TIE.2007.903939.

[27] X. Yang, Y. Fang, Y. Fu, Y. Mi, H. Li, and Y. Wang, "Low-complexity model predictive control of AC/DC converter with constant switching frequency," *IEEE Access*, vol. 8, pp. 137975–137985, 2020, doi: 10.1109/ACCESS.2020.3012163.

[28] J. Rodríguez, M. P. Kazmierkowski, J. R. Espinoza, P. Zanchetta, H. Abu-Rub, H. A. Young, and C. A. Rojas, "State of the art of finite control set model predictive control in power electronics," *IEEE Trans. Ind. Informat.*, vol. 9, no. 2, pp. 1003–1016, May 2013, doi: 10.1109/TII.2012.2221469.

[29] E. Espinosa, J. Espinoza, R. Ramirez, M. Reyes, P. Melin, J. Munoz, and C. Baier, "Finite control set—Model predictive control applied to multicell rectifiers," in *Proc. 39th Annu. Conf. IEEE Ind. Electron. Soc. (IECON)*, Vienna, Austria, Nov. 2013, pp. 5800–5805, doi: 10.1109/IECON.2013.6700085.

[30] *IEEE Standard Practices and Requirements for Semiconductor Power Rectifier Transformers*, IEEE Standard C57.18-10-1998, 1998, doi: 10.1109/IEEESTD.1998.88567.

[31] *UL Standard for Safety Dry-Type General Purpose and Power Transformers*, 4th ed., Standard UL 1561, Mar. 2011.
[32] *IEEE Recommended Practice for Establishing Liquid-Immersed and Dry-Type Power and Distribution Transformer Capability When Supplying Nonsinusoidal Load Currents*, IEEE Standard C57.110-2018 (Revision of IEEE Std C57.110-2008), Oct. 2018, pp. 1–68, doi: 10.1109/IEEESTD.2018.8511103.
[33] K. Ogata, *Discrete-Time Control Systems*, 2nd ed. London, U.K.: Prentice-Hall, 1995.
[34] P. Cortes, J. Rodriguez, C. Silva, and A. Flores, "Delay compensation in model predictive current control of a three-phase inverter," *IEEE Trans. Ind. Electron.*, vol. 59, no. 2, pp. 1323–1325, Feb. 2012, doi: 10.1109/TIE.2011.2157284.
[35] J. R. P. Cortes, "Delay compensation," in *Predictive Control of Power Converters and Electrical Drives*. Piscataway, NJ, USA: IEEE, 2012, pp. 177–189, doi: 10.1002/9781119941446.ch12.
[36] J. A. Rohten, J. R. Espinoza, J. A. Munoz, D. G. Sbarbaro, M. A. Perez, P. E. Melin, J. J. Silva, and E. E. Espinosa, "Enhanced predictive control for a wide time-variant frequency environment," *IEEE Trans. Ind. Electron.*, vol. 63, no. 9, pp. 5827–5837, Sep. 2016, doi: 10.1109/TIE.2016.2541625.
[37] J. A. Rohten, J. R. Espinoza, J. A. Munoz, M. A. Perez, P. E. Melin, J. J. Silva, E. E. Espinosa, and M. E. Rivera, "Model predictive control for power converters in a distorted three-phase power supply," *IEEE Trans. Ind. Electron.*, vol. 63, no. 9, pp. 5838–5848, Sep. 2016, doi: 10.1109/TIE.2016.2527732.

EDUARDO E. ESPINOSA (Member, IEEE) was born in Concepción, Chile, in 1983. He received the Engineering degree in electronic engineering, in 2009, and the D.Sc. degree in electrical engineering from the University of Concepción, Concepción, in 2015, with a scholarship from the Chilean Research Fund ANID.

Since August 2014, he has been with the Department of Electrical Engineering, Universidad Católica de la Santísima Concepción, Concepción, where he is currently an Assistant Professor, teaching and researching the power electronics and control systems. His research interests include model predictive control in power converters, multilevel converters, efficiency in power converters, and minimization of THD in multicell power converters.

PEDRO E. MELIN (Member, IEEE) was born in Chillán, Chile, in 1982. He received the Engineering degree in electronic engineering and the M.Sc. and D.Sc. degrees in electrical engineering from the University of Concepcion, Concepcion, Chile, in 2006, 2010, and 2014, respectively. Since 2013, he has been with the Department of Electrical and Electronic Engineering, University of Bío-Bío, Concepcion, where he is currently an Associate Professor, teaching in the areas of electronic applications and digital systems. His research interests include electronics power converters and their application, including their design, digital control, and the application of this kind of topologies to ac drives, active power filters, and energy conversion.

HUGO O. GARCÉS (Member, IEEE) was born in Talcahuano, Chile, in 1984. He received the Engineering degree in electronic engineering and the M.Sc. and D.Sc. degrees in electrical engineering from the University of Concepcion, Concepcion, Chile, in 2008, 2009, and 2016, respectively. Since March 2016, he has been with the Computer Science Department, Universidad Católica de la Santísima Concepción, Chile, where he is currently an Assistant Professor. His research interests include automation and control, instrumentation, and energy conversion.

CARLOS R. BAIER (Senior Member, IEEE) was born in Temuco, Chile, in 1979. He received the B.S., M.Sc., and D.Sc. degrees in electrical engineering from the University of Concepcion, Concepcion, Chile, in 2004, 2006, and 2010, respectively. Since 2009, he has been a Professor with the Faculty of Engineering, Universidad de Talca, Curicó, Chile, where he has been teaching in the areas of industrial electronics. His research interests include improved control techniques for multicell converters, emerging converters and strategies to inject power into the grid, and high-energy efficient improvements for medium-voltage converters.

JOSÉ R. ESPINOZA (Senior Member, IEEE) received the Engineering degree in electronic engineering and the M.Sc. degree in electrical engineering from the University of Concepción, Concepción, Chile, in 1989 and 1992, respectively, and the Ph.D. degree in electrical engineering from Concordia University, Montreal, QC, Canada, in 1997. Since 2006, he has been a Professor with the Department of Electrical Engineering, University of Concepción, where he is engaged in teaching and research in the areas of automatic control and power electronics. He has authored or coauthored more than 150 refereed journal articles and conference papers and contributed to one chapter in the *Power Electronics Handbook* (Academic Press, 2011). He is currently an Associate Editor of the IEEE TRANSACTIONS ON POWER ELECTRONICS and IEEE TRANSACTIONS ON INDUSTRIAL INFORMATICS.